6: Mineralogy

—M. Darby Dyar, Allan Treiman, Patricia Beauchamp, David Blake, Diana Blaney, Sun S. Kim, Goestar Klingelhöfer, Greg Mehall, Richard Morris, Zoran Ninkov, Ann Sprague, Michael Zolensky, and Carlé Pieters

6.1. INTRODUCTION

Minerals are described and defined not only by the elements they contain, but by the positions of the atoms relative to each other in their structures. Strictly speaking, minerals must be naturally occurring crystalline solids, since only crystalline materials can have stoichiometric elemental compositions and only crystalline materials can be phases in the thermodynamic sense, and can be placed on a stability diagram. The power of mineralogical analysis as a descriptive or predictive technique stems from the fact that only a few thousand minerals are known to occur in nature (as compared to several hundred thousand inorganic compounds), and all have specific stability ranges in pressure, temperature, and composition (PTX) space. A specific knowledge of the mineralogy of a planet's surface or interior therefore allows one to characterize the present or past conditions under which the minerals were formed or have existed. Thus, mineralogical studies are extremely well suited for characterization of planetary histories. For the purposes of this chapter, we will choose to adopt a slightly broader definition of mineralogy by including not only crystalline materials found on planetary surfaces, but also ices and glasses that can benefit from *in situ* types of analyses.

Because minerals make up the small-scale constituents of rock, they can best be studied by using *in situ* measurements. *In situ* mineralogical observations provide significant advantages over remote observations for several reasons. Perhaps the most important is that a variety of mineral-specific, mineral-sensitive techniques can be used. This permits better constraints on mineral identification and relative abundances than can be obtained from remote sensing. *In situ* measurements are made at spatial resolutions not obtainable from orbit. Mineral identification, abundance, and spatial distribution are essential for understanding formation and weathering processes.

In keeping with the theme of this volume, this chapter addresses the instrumentation needs for planetary surface exploration through two avenues. In the first section, 13 analytical techniques for mineral analysis and identification are presented, including estimates of state-of-the-art precision and current implementations of each method (Table 6.1). A brief discussion of the scientific background for each technique is presented, along with a reference list for further information of the topics tabulated here. It is hoped that this section will provide a background reference for future mission planning and instrument development.

In the second section of this chapter, mineralogical problems that can be studied with these methods are addressed. The types of mineralogical questions that can be answered on different planetary surfaces vary widely according to the type of body being studied. Due to the need to customize instrumentation for various conditions, this section is subdivided according to three different body types: primitive bodies, differentiated bodies without atmospheres, and differentiated bodies with significant atmospheres (Table 6.2, Table 6.3, and Table 6.4). Furthermore, the mineralogical questions are organized according to the types of planetary processes they address. Mineralogical studies can be used to constrain a number of planetary processes that are highlighted here: condensation, differentiation, volcanism, impact cratering, physical weathering, chemical weathering, and metamorphism. Tables in this section summarize which types of mineralogical instrumentation are needed to address which types of processes on each type of extraterrestrial body. Again, these tables are constructed to provide easy references to the instrumentation needed to address body-specific planetary processes from a mineralogical perspective.

6.2. METHODS

6.2.1. Visual Imagery at Microscales

Visual examination is among the most rapid and powerful tools for mineral identification, but is easily overlooked amid the plethora of "high-tech" spectroscopies available for robotic probes to planetary surfaces. Visual examination is the first step in mineral identification. It is taught to beginning geology students, used by professional mineralogists and petrologists in nearly all phases of investigation, and is almost always applied before more detailed or quantitative techniques (like electron microscopy, X-ray diffraction, etc.). Visual mineralogy has an honorable history in planetary exploration; it was the principal mineralogic tool on the Apollo missions and led directly to important discoveries, like "Genesis Rock" anorthosite found by the Apollo 15 astronauts. Unfortunately, robotic imaging instruments on past probes to planetary surfaces (Surveyor, Viking, Venera, VEGA) were not useful for mineralogy because their spatial resolution was too poor.

Visual examination as a mineral identification tool relies on the optical reflection properties of mineral surfaces. In effect, these properties are observed, and the observations compared with a huge database of similar observations on all known minerals (terrestrial, meteoritic, and lunar). The com-

TABLE 6.1. Analytical techniques for mineralogy.

#	Technique	Uses	Precision	Status*	References
1	Visual Imagery	Mineral and texture identification	To 100-μm scale	2	*Compton*, 1962; *Fry*, 1984; *Jakeš*, 1992; *Jakeš and Wänke*, 1993; *Thorpe and Brown*, 1985; *Tucker*, 1982
2	X-Ray Diffraction (XRD)	Mineral identification and abundance, size >0.1 mm	Identification unequivocal; abundances ~5%	3	*Bish and Post*, 1992; *Brindley*, 1980; *Clune*, 1974a,b; *Goldsmith et al.*, 1961; *Hill and Howard*, 1987; *Howard and Preston*, 1989; *Jones and Bish*, 1991; *Kastalsky and Westcott*, 1968; *Klug and Alexander*, 1974; *O'Connor and Raven*, 1988; *Post and Bish*, 1989
3	Mössbauer	Fe oxidation state and mineralogy of bulk samples Evalution of magnetic properties	1% of total Fe; 1–50% of bulk	1	*Klingelhöfer et al.*, 1995; *Agresti et al.*, 1992; *Burns*, 1993
		Fe oxidation state on microscales		5	*Agresti et al.*, 1992; *Fegley and Wänke*, 1992; *Knudsen et al.*, 1991; *Kankeleit et al.*, 1994a,b; *Klingelhöfer et al.*, 1992
4	Visible-Near-IR Spectroscopy	Abundances, cation OH stretches, CO_2 overtones, OH, H_2O, and CO_2 ions, SO_2 frosts, N ices; phase identification and abundances	To ±5% abundance	1	
5	Mid-Thermal-IR Spectroscopy	Silicate groups, composition; ionic salts; clays and hydroxyl-bearing phases; phase identification; ions and suspected glasses; thermal conductivity	Presence/absence	1	*Arnold and Wagner*, 1988; *Hapke*, 1993; *Logan et al.*, 1972; *Nash*, 1991; *Nash and Salisbury*, 1991; *Pieters and Englert*, 1993; *Sprague et al.*, 1994; *Vilas et al.*, 1984; *Wittebom and Begman*, 1984
6	Electron Magnetic Resonance (EPR, FMR)	Paramagnetic transition, metal ion abundances (FeO, Fe^{3+}, Mn^{2+}, Ti^{3+}, V^{4+}, etc.); also paramagnetic rare earth elements, radicals, defects	ppb in the lab	5	*Abragam and Bleaney*, 1970; *Hall*, 1980; *Kittel*, 1948; *McBride*, 1990; *Pinnavaia*, 1982; *Rado and Suhl*, 1963; *Tsay*, 1971; *Vonsovskii*, 1966
			ppm in flight	3	*Kim and Bradley*, 1994
7	Nuclear Magnetic Resonance	H_2O, H, OH	0.1 wt%	3	*Abragam*, 1961; *Martin and Martin*, 1980; *Pople et al.*, 1959; *Wilson*, 1987
8	X-Ray Fluorescence (XRF)	<millimeter beam size analysis of major elements	<1 mm	1	*Bertin*, 1978; see Chapter 2
9	Scanning Electron Microscope/Energy Dispersive X-Ray Analysis (SEM/EDX)	<micrometer beam size analysis of major elements; mineral form and texture	Images, 50 nm; analyses, 1 μm, ±0.5 wt%	4	
10	Raman Spectroscopy	Mineral identification, abundances	<5% abundance on 50-μm area	4	*McMillan and Hofmeister*, 1988; *Wang et al.*, 1994; *Wdowiak et al.*, 1995
11	Optical Fluorescence Spectroscopy	Mineral presence, particularly ionic salts	<5% abundance on 50-μm area	3	*Barnes*, 1958; *Geake and Walker*, 1975; *Marfunin*, 1975; *Waychunas*, 1988
12	Thermal Analysis (Differential Thermal Analysis, Differential Scanning Calorimetry)	Identification and abundances of minerals containing volatile species (OH, CO_3, SO_4) and other with phase transitions		2	See also Chapter 3
13	Magnetization (adherence to magnets of varying strengths)	Abundance and identity of ferromagnetic minerals in powdered samples	<1% of amount present	1–2	*Madsen et al.*, *Knudsen and Madsen*; *Madsen et al.*

*Status: 1 = at least one instrument flight-qualified; 5 = laboratory/concept only.

parison can be broadened to include all inorganic and organic substances and glasses. Visual examination is usually performed with some magnification because most mineral grains in rocks are too small for naked-eye examination. In the laboratory, binocular microscopes are the visual instruments of choice. In the field where space, weight, and convenience are at a premium, a hand lens of 5×–15× is the preferred tool for visual mineralogy.

The properties usually observed in visual examination are color, cleavage, fracture, luster, and habit. The property color is obvious; the human eye acts as an imaging three-color spectrometer, and can be trained to recognize subtle color differences that are strong indications of mineral identity. Fracture characterizes the morphology of broken mineral surfaces: smooth, irregular, conchoidal, etc. Many mineral species break along well-defined crystallographic directions;

TABLE 6.2. Mineralogic measurement goals: Primitive bodies.

Process	Information Desired	Measurement Goal	Instruments*
Condensation	(From pristine subsurface samples:)	A. >90% *mineral phases* identified (including hydrous phases and ices, clathrates, glasses) [1, 2, 3, 5]	A: 1–13
	1. Phase composition and zonation of silicates, ices, salts, etc.	B. Fe, Mg zonation in minerals [1]	B: 1, 8, 9
	2. Modal abundance	C. *Mineral composition*: C, N, O, Na, K, Fe, Si, Mg, Ca, Al, Ti, S, Ni of minerals to 10% of CI relative compositional abundance [1]	C: 3, 4, 8, 9
	3. Structure, crystallinity	D. *Modal abundances* to 5% [2]	D: 1, 2, 6, 7
	4. Oxidation state	E. $Fe^{2+}/Fe^{3+}/Fe^{0}$ to 5.2% [4]	E: 2, 3, 6, 7
	5. Hydration	F. *Grain size, shape, and texture* down to 10-μm scale [6]	F: 1
	6. Mineral textures and fabrics (intergrowths, overgrowths, crystal form, grain size)		
Differentiation	1. Texture of metal, silicates, and oxides (igneous?)	A. Spatial *scale of* Fe^{0} from meters to centimeters [1]	A: 1, 6, 7, 13
	2. Composition of metal, silicates, and oxides	B. Mineral phases identified [2]	B: 1–13
	3. Mg# of mafics (equilibrium assemblage?)	C. *Mineral composition*: trace-element abundance to 10% of CI: Na, K, Fe, Si, Mg, Ca, Al, Ti, S, Ni of minerals to 10% of CI relative compositional abundance [2,3]	C: 3, 4, 8, 9
		D. Grain size, shape, and texture down to 10-μm scale [1]	D: 1
Volcanism	(Vents and jets:)		
	1. Mineral assemblage and crystal form (vapor-phase condensation)	A. Mineral phases identified [1]	A: 1–13
		B. *Mineral composition*: trace-element abundance to 10% of CI: Na, K, Fe, Si, Mg, Ca, Al, Ti, S, Ni of minerals to 10% of CI relative compositional abundance [1]	B: 3, 4, 8, 9
		C. Grain size, shape, and texture down to 10-μm scale [1]	C: 1
Impact Cratering	1. Modal mineralogy (including glass)	A. *Mineral phases* identified; identify *high-pressure phases* (e.g., coesite) [1]	A: 1–13
	2. Texture and grain shape (veins, breccias)	B. Grain size, shape, and texture down to 10-μm scale [2,3]	B: 1, 2
	3. Shock and thermal effects	C. Spatial relation of glass, breccias, and mineral phases from meter to millimeter scale	C: 1
Physical Weathering	1. Grain-size distribution, melt, and lithic abundance	A. *Grain size, shape, and texture* down to 10-μm scale [1, 3, 4, 5]	A: 1
		B. I_s/FeO to 10% [3, 4, 5] (+ total Fe)	B: 3, 6
	2. Solar wind effects	C. *Spatial relation* of glass, breccias, and mineral phases from meter to millimeter scale [1, 3, 4, 5]	C: 1
	3. Soil "maturity"	D. Solar wind effects [2, 5]	D: 1, 12
	4. Depth variations	E. Detection of alteration rinds to 10 μm [2, 5]	E: 1, 3, 6
	5. Spatial variations of exposure history on meter to millimeter scale		
Chemical Weathering	1. Compositional homogeneity across grains, rocks	A. Mineral phases identified [1, 2, 3, 4]	A: 1–13
	2. P/T conditions	B. *Spatial relation* of glass and mineral phases from meter to millimeter scale [2, 4]	B: 1
	3. Rate estimates		
	4. Replacement and overgrowth textures		
Metamorphism	1. Mineral fabrics	A. Mineral phases identified [2, 3]	A: 1–13
	2. Degree of zoning	B. *Modal abundances* [3]	B: 1–7
	3. Mineral characteristics	C. *Grain size, shape, and texture* down to 10-μm scale [3]	C: 1, 2
		D. *Spatial relation* of mineral phases from meter to millimeter scale [1,3]	D: 1
		E. *Mineral composition* [3]	E: 2–6, 8, 9
		F. Fe, Mg *zonation* in minerals [2, 3]	F: 8, 9

* See Table 6.1 for a list of instruments.

this property is cleavage. The number of cleavage planes, the ease with which the mineral breaks, and other structures revealed by cleavage can be indicative or conclusive mineral identifiers (e.g., the characteristic lamellar twinning in plagioclase feldspar is best observed by the orientations of cleavage surfaces on individual twin lamellae). Luster describes the reflective properties of the surface, e.g., dull, glassy, resinous, adamantine (diamond), etc. Habit refers to the shape of a mineral grain; in many geological settings, minerals grow in characteristic shapes or crystal forms, which can be useful in their identification. These properties alone, along with some sense of the regional geological setting, are usually enough to allow mineral identification to at least group level. Equally important, the habits and relationships among mineral grains, their parageneses, can be characteristic of their conditions of formation and can constrain mineral identification. For instance, a white mineral associated with olivine could likely be plagioclase but would not likely be wollastonite.

A visual mineralogy system for a robotic probe to a planetary surface involves five elements: a source of illumination; a light input element (e.g., lens or aperture); a mobility system that allows the input element to be positioned close to the target sample; a light transfer path from the input system to the imaging sensor; and an imaging sensor element, which converts the optical image to electrical signals for storage/transmission. Each of these elements can be implemented in many ways.

TABLE 6.3. Mineralogic goals for differentiated bodies without atmospheres.

Process	Information Desired	Data	Instruments*
Condensation	1. Volatile content 2. Fe oxidation state 3. Other oxidation states 4. Elemental S content 5. Fe blebs	1.% for all measurements at *spatial scale* micrometers to meters	1–13
Differentiation	1. Mineralogic composition; evidence for fractional crystallization	Spatial *scale*: meters to centimeters	
	2. Chemical composition of rock-forming minerals pyroxene, olivine, feldspars, others (unexpected?)	Trace-element *abundance* to 2% of CI; Na, K, Fe, Si, Mg, Ca, Al, Ti, S, Ni	1–13
Volcanism	1. "Exotic" minerals and mineral assemblages (obsidian, cristobalite, tridymite, calcopyrite, wurtzite, pyrrhotite) for pressure/temperature of formation chronology of volcanism exothermic events (oldhamite, sphalerite, daubreealite)	1% abundances *Spatial scales*: micrometer to centimeter	1–13
	2. Basalts: late-stage heating to surface? Sequences that give clues to interior cooling rate 3. Grain coatings, fumarole activity, S in atmospheres, glass		
Impact Cratering	Scan crater walls for composition in variable stratigraphy	*Mineral phases* identified; *grain size, shape*, and texture to 10-μm scale Spatial relation of glass, breccias, and mineral phases from meter to millimeter scale	1–13 1
	Identify *high-pressure phase* (e.g., coesite)		
Physical Weathering	1. Size distribution of grains	*Grain size, shape, and texture* >10-μm scale	1, 9
	2. Percent glass	*Spatial relation* of glass, breccias, and mineral phases from meter to millimeter scale	1, 9
	3. Alteration rinds	*Alteration rinds* to 10 μm	9, 10
Chemical Weathering	1. Degree of cosmic-ray bombardment	*Spatial scale*: micrometer	1, 9
	2. Water of hydration	Spatial scale: micrometer and larger	2, 4, 5, 7, 10, 12
	3. Disequilibrium mineral assemblages	*Precision*: 0.2%	
	Spatial scale: millimeters to several meters		1, 4, 5, 9

* See Table 6.1 for a list of instruments.

A functional implementation is the Mikrotel instrument, which has demonstrated the feasibility and usefulness of such an imaging system (*Jakeš*, 1992; *Jakeš and Wänke*, 1993; see also Chapter 9). The Mikrotel incorporates the whole system except the mobility element in a single hardware unit; mobility is provided by a robot arm or moving vehicle (e.g., Nanokhod; see *Rieder et al.*, 1995) that positions the hardware unit over the surface of interest. The target scene is viewed through a magnifier lens group as the light input element; the choice of magnification depends on detail to be imaged (i.e., grain size of the soil or rock), and is adjustable to trade off the depth of focus and resolution. Light travels from the magnifier lens group to a commercial three-color CCD television camera through ambient atmosphere. The Mikrotel system produces good, European TV-quality (PAL) images of rock and sand surfaces and allows identification of millimeter-sized mineral grains. The Mikrotel system offers great flexibility, allowing different magnifications, imaging sensor elements, and data recording devices. In addition, the Mikrotel could be used as an imaging spectrometer if it had sensors active into near-IR wavelengths and tunable monochromatic light sources.

It is not known if the Mikrotel system is the most advantageous for robotic planetary instruments, because there have been no trade studies on possible element implementations. However, the success of the Mikrotel system appears to validate the general concept of a robotic "hand lens" as a remote system for mineral identification.

A visual mineralogy system cannot answer all questions relating to the mineralogy of planetary surfaces, but will provide rapid identification of common minerals, rapid constraints on less common minerals, and rapid guidance about which samples would yield the most return from analyses by more quantitative methods. Visual mineralogy also will supply critical constraints to assist in interpreting the results of more quantitative analytical methods (e.g., X-ray diffraction, IR reflection spectroscopy). A visual hand lens system is important or critical to field geology and regolith studies (see Chapters 8 and 9), and so appears to be among the highest priorities for development of planetary surface instruments.

6.2.2. X-Ray Diffraction Analysis

The most definitive and widely used technique of mineral identification and structural analysis is X-ray diffraction, or XRD (*Klug and Alexander*, 1974; *Bertin*, 1978; *Brindley*, 1980). When X-rays impinge on a sample, they interact with all the electrons present; most of the X-rays are scattered elastically (without change in energy). In a solid with a

TABLE 6.4. Mineralogic goals for differentiated bodies with atmospheres.

Process	Information Desired	Data	Instruments*
Condensation	See Table 6.3		
Differentiation	See Table 6.3		
Volcanism	Rock types (mineral abundances)	Grain size and shape (in rocks) Mineralogy of the phases in the rock/iron-bearing phases Volatiles in magma and their relation to atmosphere composition	1-5, 8, 10
Impact Cratering	See Table 6.3		
Physical Weathering	See Table 6.3		
Chemical Weathering	1. History of water	Hydrous phases (mineralogy, abundance, timing, distribution, and source); phase identification, 5% detection, degree of crystallinity, spatial relationships to other minerals, Fe-bearing minerals at present	1, 2, 4, 5, 7, 10, 12
	2. Presence/depth ground ice	Permafrost at depth (meters)?	See regolith
	3. History of the atmosphere	Ionic salt minerals (carbonates, sulfates, nitrates, halides, others); identification, abundances, distributions	1-13
	4. Polar processes	Clathrates, ices	1, 2, 4, 5, 9, 10, 12
	5. Hydrothermal systems	All mineral phases (volatile-bearing, impact glass, igneous minerals, hydrates, sulfates, carbonates, nitrates, Fe oxides, sulfides); identification, degree of crystallinity, abundances, distribution	1-13
Metamorphism	See Table 6.3		

* See Table 6.1 for a list of instruments.

repeating pattern of atoms (i.e., a crystal), X-rays scattered from a layer in the pattern interfere with those scattered from other layers in the pattern. When the X-rays interfere constructively, they form a *diffracted* beam of X-rays that emanates from the sample and can be detected. The directions of the diffracted beams are given by Bragg's law: $n\lambda = 2d \sin(\theta)$, where n is an integer, λ is the wavelength of the impinging X-rays, d is the distance between successive diffracting layers, and θ is half of the angle between the incident and diffracted beam directions.

If the target is a single crystal, the directions and intensities of all possible diffracted beams form the three-dimensional Fourier transform of the electron distribution (charge density function) in a unit cell of the crystal. In theory, the results of a full single-crystal diffraction experiment will yield the positions and identities of all atoms in the unit cell, the positions of bonding electrons, and the characteristics of the bonds (e.g., ionic vs. covalent). In practice, single-crystal XRD is difficult in laboratories on Earth because of the need to chose an appropriate single crystal, mount it precisely, and orient it precisely (which does not use the same X-ray detection device as taking the actual beam position and intensity measurements). The single-crystal XRD device then must be able to rotate the crystal around one axis (at least) and be able to move the X-ray detector around the crystal on two independent axes. Clearly, this analytical method is impractical as a robotically operated instrument on a planetary surface.

More commonly used (and much simpler to implement) is powder XRD, in which a powdered mineral sample is exposed to a collimated X-ray beam. The powdered sample will contain individual crystals in all possible orientations, so that X-ray intensities need only be collected around a single axis centered on the sample. In laboratories on Earth, this is usually implemented with the X-ray detector on an arm that swings around the sample in a single plane (the sample needs to be rotated around the same axis), and yields a graph or table of diffracted intensity vs. angle θ, or vs. d by Bragg's law (above). The resultant list of d values and intensities can be compared to equivalent listings from standards or known minerals (published in computerized databases such as the ICDD powder diffraction file) to identify an unknown mineral. Where the sample is a mixture of minerals, many methods can be applied to identify the different minerals (*Chung*, 1974a,b; *Bish and Chipera*, 1988; *O'Connor and Raven*, 1988; *Howard and Preston*, 1989; *Jones and Bish*, 1991). A mineral abundance of a few percent is probably the minimum detection limit for conventional powder XRD on Earth. It is sometimes possible to obtain complete mineral structures (all atom positions) from powder XRD data (*Bish and Howard*, 1986, 1988; *Snyder and Bish*, 1989; *Bish and Post*, 1993).

Powder X-ray diffraction is limited as to sample type and geometry:

1. Many crystals must be exposed to the X-ray beam simultaneously. The X-ray beam (whether from a radioactive or electrical source) is typically less than about 1 mm in diameter, so the target crystals must be small. If the target material is fine grained (e.g., wind-blown dust, soil), it may be analyzed without preparation. If the target material is coarse-grained (>50 μm), its grain size must be reduced, e.g., by a drill or grinder. Alternatively, a small single crystal can be precessed through a large number of random orientations relative to the beam.

2. Results of X-ray diffraction results may not be representative of a rock or rock unit. XRD analysis of a hand sample, even if finely polycrystalline, will characterize only its outermost hundred micrometers (approximately). Unless

the sample is broken or abraded to expose fresh surfaces, the XRD analytical volume may thus include weathering rind and powdered soil. Preferred orientation of crystals within a rock may render a rock sample unsuitable for quantitative or even qualitative analysis.

6.2.3. Mössbauer Spectroscopy

Mössbauer spectroscopy makes use of the resonance absorption of recoil-free emitted γ-rays (the Mössbauer effect) by certain nuclei in a solid to investigate the splitting of nuclear levels that is produced by interaction with its surrounding electronic environment. Resonance absorption and emission take place only under certain favorable conditions, for instance, when the absorbing (or emitting) atom is bound in a crystal lattice. In general, the nuclear energy levels of the source and absorber will be different because of different oxidation states and/or chemical environments. To achieve resonance conditions, the energy of the emitted γ-quanta has to be modulated. This is done by using the Doppler effect by mounting the source on a velocity transducer and moving it with respect to the absorber. A Mössbauer spectrum thus is the measurement of the rate of resonance absorption as a function of the relative velocity between source and absorber.

The shape of a Mössbauer spectrum is determined by the hyperfine interaction of the Fe nucleus with its electronic environment. Three hyperfine parameters can be determined by Mössbauer spectroscopy: (1) isomer shift (IS), (2) quadrupole splitting (QS), and (3) magnetic hyperfine field (Bhf). These parameters are different for different minerals. Therefore each Fe-bearing phase has its own characteristic Mössbauer spectrum. The Mössbauer spectrum of a mixture of different Fe-bearing phases is simply the superposition of the spectra of the individual Fe-bearing compounds, with the relative intensities (or relative areas) of the individual mineral spectra directly proportional to the relative amount of mineral present in the mixture. The Mössbauer parameters for individual phases are also dependent on temperature. Therefore measurements made during day and night would supply additional information.

Mössbauer spectroscopy can be performed in either transmission or backscatter geometry. In transmission geometry, the sample is placed in between the source and radiation detector and an adsorption Mössbauer spectrum is obtained. A relatively thin and homogeneous sample is needed to avoid thickness effects. Rocks could not be analyzed in this transmission-mode geometry on planetary surfaces. However, in backscatter geometry, the source and radiation detector are on the same side of the sample, so an emission Mössbauer spectrum is obtained. Backscatter geometry has no restrictions on sample shape and thickness. No sample preparation is required because the active end of the instrument is simply placed in mechanical contact with the soil or rock sample that is to be analyzed.

Major instrument parameters. Miniaturized Mössbauer instruments have been developed for use on the surfaces of the Moon or Mars (*Agresti et al.*, 1992; *Klingelhoefer et al.*, 1995). The major instrument parameters are very similar.

1. Six-detector-channel version—mass: >500 g; dimensions: ~600 cm^3; power: ~4 W; data: ~100 kb/sample analysis. Instruments of this class were included in two Discovery-class proposals for the Moon and as part of the Russian Mars '96/98 mission, installed on the Russian Mars rover "Marsokhod."

2. Two-detector-channel version (MIMOS-II)—This version was developed for use in space missions with very limited power resources, such as the Small Stations of the Russian Mars '96 mission. Mass: <300 g; dimensions: ~150 cm^3; power: ~0.5 W; data: ~60 kb/sample analysis. This instrument is shown in Fig. 6.1a and Fig. 6.1b.

For all instruments described above, a radioactive source of about 200–300 mCi of ^{57}Co (at launch) in a Rh matrix would be needed for a mission to Mars because the half-life of the source is 271 days. This lifetime has to be considered in each mission planning.

6.2.4. Visible to Near-IR Spectroscopies

Diagnostic mineral absorption bands span the near-IR, typically between 0.35 and 3.5 μm. There are two principal

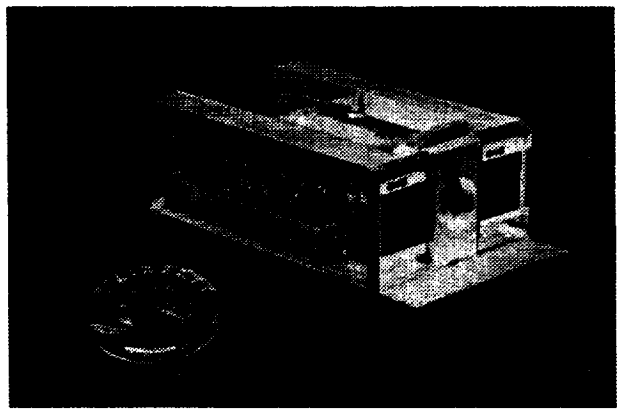

Fig. 6.1a.

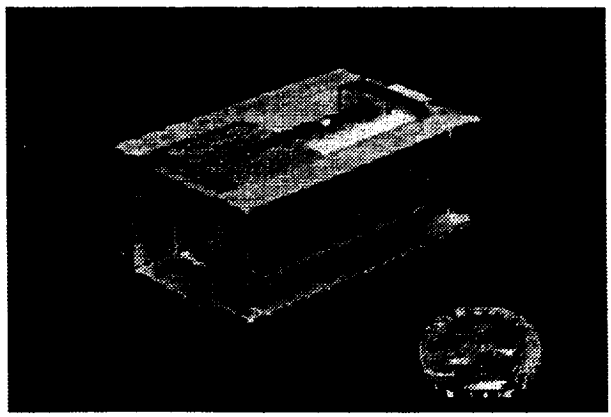

Fig. 6.1b.

causes of diagnostic features in this part of the spectrum. The first are electronic transitions of d-orbital electrons of transition element ions in a well-defined crystal field such as within an octahedral or tetrahedral site of a mineral. The energy (wavelength), strength, and width of these absorptions are a function of the ion (e.g., Fe^{+2}, Fe^{+3}, Cr^{+3}, etc.) and the size, shape, and symmetry of the site. These properties characterize specific minerals, allowing them to be identified by the nature of the observed absorption bands. Such bands are often referred to as crystal field electronic transition absorptions and occur from 0.4 to 2.5 μm. The second type of absorption bands arises from fundamental molecular vibrational and rotational modes and their overtones and combinations (typically OH, H_2O, and CO_3). These molecular absorption bands occur from about 1.4 μm to longer wavelengths.

Visible and near-IR spectrometers have a long heritage in their use for remote determination of mineralogy. The basic concept is simple: The spectral properties of light reflected from a surface are measured through a large number of contiguous spectral channels (typically a few hundred). This radiation has interacted with the surface, has been transmitted through several grains, and has obtained an imprint of absorption bands and other spectral features that are diagnostic of the minerals present. The technology developments over the last few decades have concentrated on making spectrometers more accurate, more flexible, and more capable. These trades are very important in selecting a specific design for a given application. Parallel progress has occurred in the analytical area in which tools for information extraction have been developed. These have concentrated on mineral identification, mineral abundance determination, and mineral composition determination.

Some of the most recent new technology advancements have been the development of high-precision spectrometers (imaging spectrometers) that produce "image cubes" of data: three dimensions of 10–14-bit data numbers, each with several hundred elements. Two of the dimensions contain spatial elements and the third contains spectral elements or channels. The important scientific application is the ability to evaluate diagnostic spectral properties of individual surface elements in a spatial (geologic) context. There are several spectrometer designs that will obtain image cubes, each with its own strengths and weaknesses, depending on the application. Almost all use two-dimensional arrays as the prime detector, with the third dimension derived through time-sequential measurements. If the target of interest is not moving, then the two dimensions of spatial information can be recorded simultaneously and the spectral dimension obtained sequentially with a dispersive element or filters. Alternatively, one dimension of spatial information can be recorded simultaneously with one dimension of spectral information obtained with a dispersive element or an interferogram. The second dimension of spatial information is then built sequentially as the system scans across a field of view. A more simple design is a spectrometer, which uses a dispersive element and a single or composite linear array to measure an individual spectrum; this design does require a more complex scanner to scan across two spatial dimensions.

6.2.5. Mid-/Thermal-IR

Visible and near-IR reflectance spectra are valuable in discriminating some elements and molecular groups in geologic materials, e.g., Fe, CO_3, and H_2O and OH-bearing clays and other weathering products (*McCord et al.*, 1982a,b; *Singer*, 1982; *Goetz et al.*, 1982). Many geologically important elements (like Si, Al, O, and Ca) do not absorb directly in the visible or near-IR, although they can influence the shape and location of other absorption bands (*Hunt and Salisbury*, 1970). However, many of the major rock-forming elements and their complexes have fundamental vibration frequencies corresponding to mid- and thermal-IR wavelengths, 5–50 μm. Nearly all silicates, carbonates, sulfates, phosphates, oxides, and hydroxides show mid-IR and thermal-IR spectral signatures (e.g., *Lyon*, 1962; *Hunt and Salisbury*, 1974, 1975, 1976; *Farmer*, 1974).

The strong spectral activity in the mid-IR results from structural, chemical, and physical properties of silicate rocks and minerals (e.g., *Lyon*, 1962, 1964; *Hovis and Callahan*, 1966; *Goetz*, 1967; *Lazarev*, 1972; *Farmer*, 1974; *Hunt and Salisbury*, 1974, 1975, 1976; *Karr*, 1975; *Vincent et al.*, 1975; *Salisbury and Walter*, 1989; *Walter and Salisbury*, 1989; *Hapke*, 1993; *Pieters and Englert*, 1993). *Nash et al.* (1994) give a review of mid-IR spectroscopy of the Moon. Mid-IR spectral features are characteristic of photon interactions with the material in the "transition region" where absorption bands show up as troughs in reflectance and peaks in emission. Bands in the 4–7-μm region are mostly overtones and combination tones of the stretching and bending of Si-O and Al-O fundamentals with some lattice modes present. Also, carbonates have strong absorptions from CO_3 internal vibrations in the 6–8-μm region; these bands are easily distinguished from silicate absorptions (*Adler and Kerr*, 1963; *Hunt and Salisbury*, 1975).

The 7–11-μm region is largely dominated by surface scattering except at the Christiansen frequency or feature (CF). The CF is a reflectance minimum (and corresponding emittance maximum), typically between 7 and 9 μm, representing the strongest molecular vibration absorption band in silicate rocks and minerals. The CF wavelength is a function of the polymerization of the silicate lattice, and so is diagnostic of rock type and the chemical compositions of minerals (*Vincent and Thomson*, 1972; *Hunt and Salisbury*, 1974; *Hunt*, 1980). Glassy and powdery samples yield more subdued spectral features than crystalline or slab samples, at least in the laboratory, but the CF wavelength is independent of grain size or texture. Emission spectra obtained by telescope or method are approximately the "complement" of reflectance spectra as given by Kirchhoff's Law: fractional absorptivity = 1 – the

fractional reflectivity. Note also that, in strict thermodynamic equilibrium, fractional emissivity = fractional absorptivity.

Infrared spectral features at wavelengths longer than 11 μm are "transparency features"; quartz and feldspar have strong and unique features in this region. Several examples are given in the laboratory compendia of Salisbury and others (see reference list). The features in the 12–40-μm range include Si, O, and Al stretching and bending modes. Hydroxide-bearing minerals (clays) also have characteristic mid-IR spectra (*van der Marel and Beutelspacher*, 1976), with spectral features from the fundamental bending modes of OH attached to various metal ions, such as an H-O-Al bending mode near 11 μm in kaolinite (*Hunt*, 1980). Phosphates and sulfates also have diagnostic absorption bands associated with their anion complexes (PO_4^{3-} and SO_4^{4-}), as do oxides, nitrites, and nitrates. Sulfides and halogenide salts are also readily distinguished (*Hunt and Salisbury*, 1975).

For natural surfaces, thermal emission spectra are modified by scattering of the outgoing energy within the surface. Thus, physical properties such as particle size and packing can affect emission spectra (*Logan et al.*, 1973; *Salisbury and Estes*, 1985; *Salisbury and Walter*, 1989). These effects only become significant as the particle size becomes small (<~100 μm) and are most important as the size approaches the wavelength being observed (*Lyon*, 1964; *Hunt and Vincent*, 1968; *Hunt and Logan*, 1972; *Salisbury and Walter*, 1989). To deal with the effects of scattering, the thermal emission data can be modeled using radiative transfer techniques that incorporate Mie scattering theory (*Conel*, 1969; *Moersch and Christensen*, 1991), and Chandrasekhar scattering theory (*Hapke*, 1981).

For airless body studies like Mercury, asteroids, and the Moon, the diagnostic utility of the mid-IR spectral regions benefits from the vacuum environment surrounding the surface materials, which enhances spectral contrast over that obtained in laboratory spectra most commonly obtained at ambient 1-bar pressure. For Mars, the atmospheric emission spectrum will mix with that from the surface materials. Mars Observer carried the thermal emission spectrometer (TES) on board for planned surface and atmospheric studies.

One thermal emission spectrometer design is flight-qualified, flew on Mars Observer, and is slated for the Mars Global Surveyor mission (*Christensen et al.*, 1992). That instrument, the TES, weighs 14.4 kg and consumes 14.5 W on average. Individual mineral species were clearly distinct in their thermal emission spectra, such that a grain of olivine could confidently be distinguished from pyroxene. Mineral mixtures could also be discriminated. Sulfates were detectable at a few weight percent (*Christensen et al.*, 1992), but it is not clear how well silicate mixtures could be discriminated.

6.2.6a. Electron Paramagnetic Resonance (EPR)

Electron paramagnetic resonance (EPR) or electron spin resonance (ESR) spectroscopy studies atoms, ions, or molecules with unpaired electron(s) in an applied magnetic field (e.g., 1–6 kG) by irradiation of microwaves (~9 GHz for X-band EPR) to induce transitions between electronic spin states. The electronic states and their energy levels are modified through various interactions, such as interaction with nuclear spin(s) (within the same atom or molecule or neighboring ones), molecular environment, or amorphous or crystalline matrix. Magnitudes of such interactions can be deduced through EPR spectra and used to obtain information about molecular structures of radicals, oxidation states of ions, electronic structures, symmetry of ionic sites, and the surroundings. Samples of all phases, gas, liquid, or solid, can be studied by EPR. In conventional EPR experiments, the microwave frequency is fixed at a tuned value, and resonance condition is searched by scanning the applied magnetic field through an electromagnet.

EPR has been extensively applied for the study of geologic materials of all phases, including crystalline, powder, and amorphous samples. The analysis can be carried out with little disruption of surface structures or chemical equilibria, and requires little sample preparation, with milligram- to gram-sized samples.

Specific applications of EPR for planetary exploration include: the nature of oxidant (radicals) in martian soil; oxidation state of paramagnetic ions in soil (mineralogy); characterization of volatiles (carbonates, sulfates, nitrates); color centers in icy samples (impurity level chemicals in ice, inorganics, organics, carbonates); and detection of possible organics from subsoil.

6.2.6b. Ferromagnetic Resonance (FMR)

Compared with the paramagnetic samples in which individual electron spins are isolated or weakly interacting, the spins in ferromagnetic samples, e.g., metals of Fe, Co, and Ni and some rare-earth elements, are strongly coupled and possess a spontaneous magnetic moment even in the absence of an applied magnetic field. Spectroscopic principles and instruments are the same as EPR, except that in the interpretation of spectra, the ferromagnetic nature of the samples must be considered. Detection and characterization of ferromagnetic particles are the most important applications of FMR for planetary exploration.

6.2.7. Nuclear Magnetic Resonance (NMR)

Nuclear magnetic resonance (NMR) studies atoms or molecules with nuclear spin(s); in most other aspects, its principles of operation are similar to those of EPR. NMR exploits the fact that many isotopes in molecules possess unique nuclear gyromagnetic ratios. Through interactions with electrons and neighboring nuclei, NMR spectra of molecules show unique line shapes or chemical shifts, and such information is utilized for characterization purposes. Through NMR spectroscopy, one can obtain information about the constituent nuclei and chemical structure of molecules. From the time of inception, the proton has been the most frequently studied nucleus and thus proton magnetic resonance has

become almost synonymous with NMR. Using proton-NMR, one can accurately determine the quantity and physical and chemical nature of water, i.e., H_2O, OH, in geologic samples. Proton NMR is operated with samples (0.1–1 g) in an applied magnetic field by irradiation of radiofrequency (e.g., ~13 MHz at ~3 kG) to induce transitions between proton spin states.

NMR can be obtained by scanning a magnetic field at a fixed radiofrequency or by scanning radiofrequency at a fixed magnetic field. Like EPR, the method is nondestructive, and requires little sample preparation. A miniature magnetic resonance spectrometer (<500 g, <5 W) with combined capabilities of EPR and NMR is being developed at JPL (*Kim and Bradley*, 1994). A permanent magnet assembly (Nd-B-Fe) is used for the spectrometer.

Specific applications of NMR for planetary exploration include the presence of water in the soil, minerals, and rocks; free water in rock pores; adsorbed water on surface; and chemically bound water.

6.2.8. X-Ray Fluorescence Analysis (XRF)

XRF is principally a bulk chemical analysis method, and is described in Chapter 2. However, bulk chemistry of single mineral grains can provide important clues to their identity; when coupled with other structural data, identification is almost assured. One proposed instrument that uses XRF primarily as a mineralogic tool is under development. It is designed to analyze powder samples in a transmitted, forward reflection geometry either as received (e.g., wind-blown dust) or as the result of grinding or drilling operations (David Blake, personal communication). This instrument would yield bulk composition and X-ray diffraction data simultaneously. This instrument is proposed for inclusion on the Champollion lander and the Mars '98 missions. Its principal engineering parameters are energy range: 150–8050 eV; diffraction range (2-θ) 5–50; X-ray source: copper anode X-ray tube (or radioactive source, where appropriate); detector: 1024 × 1024, 18 μm pixels CCD; size: 11 × 11 × 8 cm; mass: 800 g; power (operating): 3 W; energy per sample: 6 W-h.

6.2.9. SEM/EDX

A scanning electron microscope with chemical analytical capability using energy dispersive analysis (SEM/EDX) could be useful in mineralogy as a source of morphological and compositional data on individual mineral grains. SEM/EDX is briefly discussed in Chapter 2.

6.2.10. Raman Spectroscopy

Laser Raman spectroscopy is an optical scattering technique that can provide molecular and crystal-structural information about solid materials (*McMillan and Hawthorne*, 1988; T. Wdowiak, personal communication). Raman spectroscopy is an established laboratory method for identification and characterization of organic/hydrocarbon and inorganic/mineral substances (e.g., *Wang et al.*, 1994). When light interacts with a material, a small portion of the incident photons (one photon per 10^8–10^{12}) is scattered inelastically, with energy loss/gain to/from the material; this is the Raman effect. The energy losses or gains associated with Raman scattering are characteristic of molecular and lattice vibrational modes (fundamental, combination, and overtone) of the target material, and can be used to identify and characterize the target material.

The spectral frequency shifts of Raman scattering are related to molecular structures in essentially the same way as the absorption/emission transitions in infrared absorption, reflectance, and emission spectroscopy; however, different transitions are observed by the two techniques, as the quantum selection rules are different for absorption and Raman scattering. Additionally, many of the common difficulties in interpreting infrared spectra such as particle size effects, transparency peaks, volume scattering, and thermal gradients are not problems in Raman. Instead of the broad absorption bands of visible and infrared spectra, Raman spectra record discrete, sharp emission peaks. Laser-light-induced fluorescence of some species can be an interference, but techniques are available for minimizing its effect. These include algorithms for extraction of the narrower Raman features, long-wavelength lasers that induce less fluorescence, and time gating of the detector that excludes fluorescence because of its longer duration.

Raman spectra are taken by illuminating the sample with a monochromatic light source and obtaining spectra at wavelengths longer (and shorter) than that of the source. In the laboratory, Raman spectra of solids are usually obtained on prepared powders, although spectra can also be obtained on individual mineral grains through an optical microscope ("micro-Raman" spectroscopy). The analytical depth is effectively the depth of light penetration into the solid.

The Raman spectrometer consists of five components: laser light source, absorption filter (notch) at the light source wavelength, monochrometer, optical coupling, and detection (CCD) system. The light source must be monochromatic, and laser diodes are suitable. Single-mode laser diodes with efficiencies of 23–40%, power draws of 3–500 mW, and wavelengths of 630 nm or longer are suitable sources for Raman spectroscopy. Light can be conducted to the sample by a fiber-optic cable. The filter and monochrometer prevent all light with wavelengths near that of the incident light from hitting the detector. Holographic notch filters at laser wavelengths of sufficient absorption efficiency are available for this purpose commercially. Light scattered from the target material must be conducted to the detector. The monochrometer and detector can be at the site of analysis, or the light can be conducted by fiber-optic cable from a remote sample to the monochromator/detector system. Cables of sufficient clarity and length (up to 1 km) are available commercially (*Schoen*, 1994); temperatures as low as 77 K can be tolerated. Finally, the monochrometer must be able to disperse light by wavelength

and the detector must record a spectrum of sufficient signal/noise. Available CCD spectrometer systems of small size and weight are apparently adequate for this task.

While Raman spectroscopy is a powerful laboratory technique, its value in robotic sensing of planetary surfaces (*Wdowiak et al.*, 1995) remains to be validated through actual testing. The low efficiency of Raman excitation implies low signal/noise in the detector, and requires either long analysis times, high-power light sources, or both. Stimulated Raman spectroscopy (*McMillan and Hofmeister*, 1988) permits much higher excitation efficiencies, but at the cost of large power flux and sample heating. Once a Raman spectrum is obtained, it is not clear how well spectra of mineral mixtures can be deconvolved to yield species or abundances of the constituent minerals, and what the minimum detectable mineral abundance is. The answer may lie in the use of microscopic Raman spectroscopy on single mineral grains, a standard laboratory technique. However, Raman spectra can readily distinguish crystalline and glassy materials, a difficult task for most methods. These questions are obvious points for future research in this promising technique.

6.2.11. Optical Luminescence Spectroscopy

Optical luminescence is emission of nonthermal optical photons (near-UV through IR) as a response to energy input (*Barnes*, 1958; *Geake and Walker*, 1975; *Marfunin*, 1975; *Waychunas*, 1988). On absorption of energy, an atom (or ion) will enter an excited state; the most probable decay mechanism of many such excited states involving valence-band electrons is emission of an optical photon.

Fluorescence is prompt emission in response to high-energy photons, and can be useful in determinative mineralogy, especially of ionic salts (e.g., carbonates, sulfates). Fluorescence can arise from essential elements (or ions), trace-element substituents (activators), or defects. Common activators in salts of alkali and alkaline earth elements include Mn^{2+}(VI), other transition metals, the rare earths, and the actinides (*Waychunas*, 1988). Trace substituents of other species can enhance fluorescence (e.g., Pb^{2+}), while other species (e.g., Fe^{3+}) quench it effectively. Fluorescence can also arise from defects in crystal structures, including those caused by radiation and shock.

Minerals may also luminesce on heating, thermoluminescence (TL), as structural defects like radiation damage anneal out. Thermoluminescence can be readily related to radiation exposure, and a suitable heating chamber [like a differential scanning calorimeter (DSC)] may be available on the lander.

Optical luminescence may be particularly useful for surface investigations on Mars, as atmosphere-surface interactions may have produced ionic salts of the alkali and alkaline earth elements (*Gooding*, 1978, 1992; *Sidorov and Zolotov*, 1986; *Fegley and Treiman*, 1992; *Treiman*, 1992; *Treiman et al.*, 1993). One possible Mars surface mineral, scapolite, has distinctive optical luminescence, and should be readily detectable (*Clark et al.*, 1990; *Treiman*, 1992).

Instrumentation to permit fluorescence spectroscopy is simple: a VIS-NIR spectrometer and a short-wavelength light source. The former is likely to be manifested for reflection spectroscopy, and the latter might be manifested for other purposes (e.g., a laser range finder, atmosphere sounder, or chemical analytical tool). However, fluorescence spectroscopy has severe limitations, and cannot be considered a mature analytical method. In most cases, fluorescence spectroscopy cannot provide mineral proportions or compositions, as luminescence response of a mineral depends on many aspects of its trace-element composition and structural state. Also, there has been little systematic investigation of luminescence at infrared wavelengths or of faint luminescences (that interfere with Raman spectroscopy). This is a field with considerable potential, as many common minerals that do not luminesce at visible wavelengths may do so in the infrared.

6.2.12. Thermal Analyses

Many minerals transform or react during heating, and the thermal effects of those transformations can be characteristic of particular minerals, and nearly unequivocal for mineral identification. These thermal effects are the basis for the standard thermal methods, which include differential thermal analysis (DTA) and differential scanning calorimetry (DSC). In both methods, an unknown sample is introduced into a heating chamber in close proximity to a reference sample, and both sample and reference are heated. In DTA, heat is added to sample and reference at a constant rate (usually linear with time) and the temperature difference between the sample and reference is recorded. In DSC, sample and unknown are heated separately so that both stay at the same temperature; the recorded quantity is the difference in heat added as a function of reference temperature. DSC can be more quantitative that DTA with respect to the abundances of phases (the heats absorbed or evolved); this quantification, however, requires accurate masses of the analyzed samples. DSC also is currently limited to thermal effects below 700°C (*Wendlandt*, 1986). DTA is semiquantitative with respect to mineral abundances, but is easier to implement than DSC and is limited only to temperatures below 1200°C (*Wendlandt*, 1986).

Thermal analysis (DSC or DTA) by itself can detect the heat effects associated with crystalline phase changes, magnetic order/disorder transition, chemical reactions such as devolatilizaton, and melting. However, thermal analysis techniques are especially powerful when coupled with a method of analyzing the gas (if any) emitted during a thermal event. There are many available methods for analyzing the gases evolved during heating. Mass spectrometric methods are discussed in Chapter 3. Gas chromatography (GC), also discussed briefly in Chapter 3, involves passing the evolved gas in an inert carrier through a long column of porous, chemically adsorbing material. As they pass through the column, the evolved gas species become separated according to how well they bind to the column material. Properly cali-

brated, GC can be nearly definitive for presence and abundance of some species. For samples that contain only a few known volatile species, or for applications where concentrations of only a few species are needed, gas-specific chemical sensors are favored. Most compound-specific sensors are designed so the compound of interest sets up an electrochemical potential (voltage) across the sensor; the potential is a calibrated function of the compound abundance. Many compound-specific electrodes respond (to varying degrees) to nontarget compounds, so sensors for a number of specific compounds may be required to yield unambiguous analyses. For water, other types of sensors can measure relative humidity or dew point. Sensors for H_2O and CO_2 were available in 1994 (*Boynton et al.*, 1994; *Gooding*, 1994), and development of other compound-specific sensors is in progress.

This combination of methods, thermal and evolved gas, can provide significant mineralogical information about unknown samples, including mixtures and complex soil samples (*Wendlandt*, 1986). Thermal/evolved-gas methods are particularly powerful for volatile-rich materials, such as terrestrial soils. Their analytical values presumably extend to martian soils, regoliths of primitive asteroids, and regoliths of comets. Thermal analysis is a bulk technique for the sample collected; it is not sensitive to surface coatings and weathering rinds (*Schwartz et al.*, 1995), except as the coatings and rinds become a significant portion of the sample mass. With thermal analysis and evolved gas analysis, it is relatively straightforward to distinguish among clays, silicates, feldspars, zeolites, glasses, and evaporites as well as to determine if organics are present, even for some phases to the 0.02 wt% level (*Boynton et al.*, 1994). Thermal and evolved gas methods are also discussed in Chapters 3 and 7 as they relate to trapped/implanted gases and C-based chemistry/exobiology.

No thermal analysis instruments are currently flight qualified, but a number are at brassboard stage, and are competing for inclusion in the Mars Surveyor Lander. Current concepts couple thermal analyses with evolved gas analysis: *Mancinelli et al.* (1994) proposed a DTA with a evolved gas analysis by chromatography; *Boynton et al.* (1994) and *Gooding et al.* (1994) have proposed DSCs with evolved gas analysis by compound-specific sensors. Gooding et al.'s instrument (TAPS) has a mass near 1 kg, including a sampling device, and consumes ~5 W-hr per analysis of a 20–50-mg sample. Minerals with thermal effects alone (e.g., quartz) are detectable at near 1% of the sample. Minerals that evolve gas may be detectable at much lower levels (e.g., carbonate detectable at the 0.02% level).

6.2.13. Magnetization

A remarkable result from the Viking missions was the discovery that the martian soil is highly magnetic, in the sense that the soil is attracted by a small permanent magnet. The soil was found to adhere almost equally to a strong and a weak Sm-Co magnet attached to the Viking lander backhoe at both landing sites. The strong magnet had a surface field and a surface field gradient of 0.25 T and 100 T/m respectively (2500 G, 10,000 G/cm). The corresponding numbers for the weak magnet were 0.07 T and 30 T/m (700 G, 3000 G/cm). Based on the returned pictures of the amount of soil clinging to the magnets, it was estimated that the particles in the martian dust contain between 1% and 7% of a strongly magnetic phase, most probably a ferrimagnetic ferric oxide intimately dispersed throughout the soil.

Appropriate limits for the spontaneous magnetization (ss) were advanced:

$$1\ \mathrm{Am^2(kg\ soil)^{-1}} < \mathrm{ss} < 7\ \mathrm{Am^2(kg\ soil)^{-1}}$$

The essential difference between Permanent Magnet Arrays for coming landers and the Viking Magnetic Properties Experiment is that arrays on future landers should include magnets of lower strengths than the weakest Viking magnets. The reason for this is that both the strong and weak magnets on the Viking Landers were saturated with dust throughout the mission. The proposed Magnet Array contains five magnets of different strengths, with a total mass of about 70 g. The outer diameter of the magnets is 18 mm each. The center and ring magnets are magnetized parallel to their axes, but in opposite directions. When mounted the magnets are completely immersed in a thin Mg plate. The magnets are of equal strengths, but mounted at different depths below the surface of the Mg plate. Discrete (single-phase) particles of the strongly magnetic minerals (γ-Fe_2O_3, Fe_3O_4) will stick to all five magnets, while composite (multiphase) particles will stick only to the strongest magnets. The two strongest magnets have the same strengths as the backhoe magnets on the Viking landers. The plate with the magnets will be placed on the surface of the lander. The Magnet Array will be periodically viewed by the onboard camera and the returned pictures are the data on which conclusions will be based. If the Magnet Array is placed on the surface of the lander, it will be possible to perform X-ray fluorescence and Mössbauer analysis of the dust on the magnets.

6.3. PRIMITIVE BODIES

The many different types of undifferentiated bodies in the solar system share a collection of surficial and interior processes that can be profitably studied by determining the mineralogy of reactant and resultant phases. The types of processes and the unique instrumentation required to address them are presented in Table 6.2. Specific issues for each type of body are further (briefly) summarized here. First, the reader should recognize that the basic types of undifferentiated bodies are somewhat arbitrarily divided into (1) asteroids and (2) comets and Kuiper Belt objects. While the latter are assumed to be the more primitive, in reality there is a complete gradation between these objects and their effective discrimination hinges on the presence or absence of an ephemeral atmosphere. The analysis concerns with regard to mineralogy are similar for all primitive bodies.

The key questions for primitive bodies focus on the recognition and identification of interstellar, nebular, and protoplanetary minerals, and the phases resulting from oxidation, sulfidation, heating (and further crystallization of amorphous materials), carburization, and aqueous alteration state of the primary materials. Some primitive phases are known to be amorphous, and subsequent heating and annealing will produce materials with a varying degree of crystallinity. For this reason, techniques that can probe atomic structure (X-ray diffraction, Mössbauer, optical spectroscopy, differential scanning calorimetry) will be critical tools. The oxidation state of minerals and bulk samples is also critical information, and this can be analyzed by Mössbauer, electron magnetic resonance, and visible-NIR spectroscopic techniques. Major-element compositions can be probed using SEM/EDX and XRF instruments. Mineral textures are important records of formation processes, and these can be studied using SEM or visual imaging techniques.

6.4. DIFFERENTIATED BODIES WITH NO (OR NEGLIGIBLE) ATMOSPHERES

The many different types of differentiated bodies in the solar system that lack significant atmospheres share a collection of surficial and interior processes that can be studied using mineralogy. The types of processes and the unique instrumentation required to address them are presented in Table 6.3. Specific issues for each type of body are further (briefly) summarized here.

On Mercury, key mineralogical questions focus on the oxidation state of the surface mineralogy and the composition of the polar deposits. In the former case, mineralogy (which is dependent on knowledge of oxidation state) of surface sulfides may give significant insight into the oxidation state of the planet at the time of formation and core formation. Related to this is the Mg/(Fe + Mg) ratio, a parameter that places important constraints on petrology but cannot be evaluated because the oxidation state is not known. In the latter case, knowledge of the composition of the polar deposits on Mercury can yield important insight into volatiles and differentiation on the planet. Finally, knowledge of the Na content of feldspar on Mercury's surface could provide constraints on surface evolution.

On the Moon, we note that the Apollo program, groundbased observations, and Clementine have been effective in studying the composition of the lunar surface. Thus, these authors believe that more emphasis should be placed on other airless bodies in this document. However, key issues that have not been explored to date include knowledge of the composition of polar deposits, and sampling of xenoliths or deep craters to attempt to sample the lunar mantle.

For differentiated asteroids, mineralogy could provide knowledge of the surficial evolution by determining the presence or absence of hydrated minerals, the elemental abundances at the surfaces, and any mantle signatures that might be present. Finally, for Galilean and saturnian satellites, the surface mineralogy and bulk composition are again important. For these bodies, such information could provide insight in the fractional amount of water on the surfaces, other imbedded gases, dimers, molecules, and the rates of sputtering, outgassing, and accretionary processes present.

6.5. DIFFERENTIATED PLANETS WITH ATMOSPHERES

The surface mineralogy of differentiated planets with atmospheres (i.e., Venus and Mars) differs dramatically from that found on primitive bodies and differentiated planets that lack an atmosphere, and therefore deserves more extensive discussion herein. The types of processes and the unique instrumentation required to address them are presented in Table 6.4.

Rock-atmosphere-hydrosphere interaction on Mars and rock-atmosphere interactions on Venus have undoubtedly led to a wide variety of minerals that reflect specific processes that have occurred. These interactions are broadly called "chemical weathering" because the initial mineralogy of the source rock has been changed. Because mineral phases are stable only for specific ranges of pressure, temperature, and composition, the mineralogy of the alteration products and their spatial and petrologic associations provide insight into the environments in which they formed. In this context, it is important to note that minerals, once formed, can persist metastably for extended periods of time.

In the case of Mars, for example, hydrated minerals formed early in its history could persist to the present time under the cold dry conditions that prevail now. Surface mineralogy can also provide information critical to the exobiological exploration of Mars.

There are two principal reasons for this. First, life as we know it requires liquid water, and a knowledge of surface mineralogy provides insight into the activity of water. Second, the biogenic elements H, C, N, O, and S are also the principal volatile elements comprising the present and past atmospheres of Mars. In this section, we attempt to present a sampling of the critical questions that can be answered if surface mineralogy is known.

6.5.1. Chemical Weathering

Throughout the last 4 b.y. the atmospheres of Mars and Venus has been interacting with the surface to alter initially igneous material. Minerals are a permanent reservoir of CO_2 and S for both Venus and Mars and for H_2O on Mars. Elemental abundances, such as those measured by the Viking XRF experiment, can constrain the present state and allow inference of the starting composition of the source material but not reveal the processes that have occurred. The mineralogy of the alteration products is a sensitive indicator of formation conditions such as oxidation state, pH, abundance and phase of water, atmospheric chemistry, temperature, and surface

pressure. This knowledge is critical in understanding the Mars and Venus volatile cycles during the present epoch and throughout the planets' history.

Types of secondary minerals that are especially important are sulfates, carbonates, Fe oxides, and, on Mars, where water has been involved in weathering the environment, hydrates. In addition to determining the mineralogy of the weathering product, the mineralogy of unaltered material needs to be determined. We need to know the mafic mineralogy of the source rock (e.g., olivine and pyroxene composition and abundance) in order to separate weathering products derived locally under current conditions from material formed under other conditions. Contextual information such as the composition of any weathering rinds on rocks and how it differs from soil mineralogy and the mineralogy of any duricrusts is needed to derive an integrated picture of what processes have occurred and when.

For instance, consider weathering under current martian conditions. Two weathering paths may be occurring. The first is gas-solid reactions at 240 K, while the second assumes that occasional films of liquid water are present at 273 K (applicable in the equatorial regions). Using mineral reaction diagrams, the thermodynamically stable alteration products for each reaction path can be determined (*Gooding*, 1978; *Gooding and Keil*, 1978; *Gooding et al.*, 1992). For gas-solid reactions at 240 K the dominant weathering products are clays (including the smectite Ca-beidellite) and the carbonates magnesite ($MgCO_3$), dolomite [$CaMg(CO_3)_2$], or calcite ($CaCO_3$).

With liquid-solid reactions at 273 K in addition to the minerals mentioned for solid-vapor interactions, Mg-phyllosilicates (talc, saponite, and montmorillonite) and (Na,K) beidellites would be present. The composition and abundance of currently formed alteration products provides a mechanism to estimate the rate at which H_2O and CO_2 are being removed from the martian atmosphere-cap regolith cycle today.

Another martian example is that the mineralogy of weathered materials formed during an early clement period on Mars where liquid water was abundant would be rich in carbonates. Dissolved CO_2 in water would react quickly to form massive carbonate deposits (e.g., *Fanale and Cannon*, 1979; *Pollack et al.*, 1987). The abundance and mobility of water during this period would determine the mineralogy of the clays based on the solubility of different ions.

Sulfur is fairly abundant on the martian surface; soils analyzed by both Viking Lander XRF instruments contained 5–9 wt% SO_3. The elemental analyses of the red fine-grained material that dominated the surface at both sites were nearly identical for most elements, except S, whose concentration was variable in the different soil samples collected at the two sites (*Clark et al.*, 1982). The oxidation state of the surface and the concentration of S in clods was interpreted as a sulfate duricrust formed by the upward migration of water containing the sulfate anion (*Toulmin et al.*, 1977; *Burns*, 1988) or alternatively deposited from volcanic aerosols (*Settle*, 1979). Knowledge of the mineralogy and distribution of martian sulfates is critical in determining how the duricrust formed.

Understanding the nature of chemical weathering on Mars cannot be done without knowing the mineralogy of Fe. This is the case because it is abundant on the martian surface (~12% Fe according to *Clark et al.*, 1982), forms stable compounds in both divalent and trivalent oxidation states, and changes oxidation state in response to external conditions. Arguments developed by *Morris et al.* (1989) and *Morris and Lauer* (1990) suggest that well-crystalline hematite (α-Fe_2O_3) is present as an optically important constituent on Mars. This may imply that the surface of Mars is anhydrous and/or that formation process were at high enough temperatures to form hematite relative to ferric oxyhydroxide phases. It is also important to establish the size distribution of Fe oxide particles. Small particles (nanophase ferric oxides) are formed during low-temperature processes like palagonitization, and well-crystalline ferric oxides are formed by higher-temperature hydrothermal processes.

On Mars, the alteration of material in impact ejecta blankets or volcanic geothermal regions would also have a distinctive geochemical signature due to the circulation of hydrothermal fluids interacting with impact glasses and breccias. Calculations based on minimizing the Gibbs free energy of the chemical system by *Zolensky et al.* (1988) show that gibbsite ($Al(OH)_3$), kaolinite (an Al-rich clay), and nontronite (an Fe-rich smectite clay) would be present. The abundance of each clay would depend on the amount of rock that has reacted and the initial composition of the rock. If only a small percentage of the rock reacts, carbonates would not form.

6.5.2. Importance of Mineralogy for the Exobiological Exploration of Mars

According to a recent study document (*Carr et al.*, 1995, "An Exobiological Strategy for Mars Exploration"), three scenarios exist that are of high exobiological interest: (1) Prebiotic organic chemistry occurred but life never developed; (2) life developed in some form during an earlier clement period but is now extinct; and (3) life exists, perhaps in "clement" niches in or below the surface.

Unless one assumes that life forms were delivered to Mars from elsewhere, (1) above is required for (2) and (3), and evidence of (2) is likely to exist in the rock record if (3) is true. The Viking life detection experiments revealed the presence of a strong oxidant in the Mars soil that could have destroyed any evidence of organic materials. It appears that, until much more is known about the geology, mineralogy, and surface chemistry of Mars, exobiological investigations should be undertaken that have the broadest possible scope.

6.5.3. Early History of Martian Volatiles

Mars is a dry eolian planet with a tenuous atmosphere of ~7 mbar pressure, composed mostly of CO_2. However, ancient surface morphological features such as stream channels

and other fluvial and lacustrine features provide compelling evidence that liquid water once existed on the surface of Mars in large quantity. This abundance of liquid water implies that early Mars was once wetter and warmer, and had a dense atmosphere, perhaps of a greenhouse gas such as CO_2 (*Clifford et al.*, 1988). The ultimate fate of atmospheric CO_2 is of exobiological interest because this compound figures prominently in prebiotic organic chemistry, and because a full inventory of the CO_2 sinks is required to provide a balanced volatile budget for the planet. A major reservoir for the CO_2 could be in the form of carbonates deposited as chemical sediments or as hydrothermal precipitates.

Alternatively (or additionally), CO_2 could be stored in the form of clathrate hydrates beneath the surface or in the polar caps (*Miller*, 1973), or as solid CO_2 at the poles. Each of these phases can be unequivocally distinguished and characterized by mineralogical techniques. In the case of carbonates, the crystal symmetry (rhombohedral or orthorhombic) and the extent of cation solid solution (Ca, Mg, Fe, Mn, etc.), cation order/disorder, and cation stoichiometry can all be determined through mineralogical analysis.

Each of these distinguishing characteristics provides information about the specific origin of the mineral phase and its environment of formation. The total quantity of water that apparently existed on the surface of Mars early in its history cannot be accounted for by the polar caps alone. It is likely that hydrated phases exist either as a consequence of their direct deposition from aqueous solution or as products of the reaction of anhydrous igneous minerals with water. The quantity, type, and degree of crystallinity of clays, micas, and other hydrated phases can be determined by mineralogical analysis and their known stability relationships can constrain the conditions under which they were formed.

6.5.4. Presence and Lateral Extent of Hydrothermal Systems

Abundant morphological evidence exists for early and extensive volcanic activity on the surface of Mars, and for the presence of liquid water. The juxtaposition of these features is permissive if not compelling evidence that hydrothermal systems once (or have always) existed on Mars. Isotopic data from the SNC meteorites also suggests that there was an exchange of H and O between the crust and the atmosphere. The depletion of volatiles such as S and C is puzzling, and these elements may now be contained within minerals precipitated in hydrothermal systems. A knowledge of the presence and distribution of S and C containing mineral phases is important first because they are biogenic elements, and second because compounds containing them could have been utilized by autotrophic organisms as energy sources. Ancient hydrothermal systems could have been eroded or exhumed, exposing minerals and mineral assemblages at the surface that were formed at depths inaccessible in presently active systems. The mineralogical characterization of such a system could provide an evaluation of the role hydrothermal processing has played in modifying the early martian atmosphere and in altering deep-seated volcanic rocks. Hydrothermally altered rocks, dissected and exposed at the surface by erosion, could contain fossil evidence of the nature of the early Mars atmosphere and of the fate of its volatiles.

6.5.5. Evidence of Prebiotic Organic Chemistry

On the Earth, all evidence of prebiotic organic chemistry has been erased. In the earliest terrestrial rocks for which conditions of metamorphism would permit it, evidence of life is present. Therefore, even if life never originated on Mars, it would be exceedingly valuable to find some evidence in the geologic record of martian prebiotic organic chemistry. This would be possible on Mars more than on the Earth, since extensive regions of ancient terrain exist on Mars that have not been subject to metamorphism. The current notions of prebiotic organic chemistry are that many important reactions may have occurred in hydrothermal systems where energy could have been provided by mineral hydration reactions. Hydrothermal systems also provide a means for gas exchange with the atmosphere and transport of reactants to the sites of reactions. Ancient hydrothermal systems exhumed by erosion could provide surface material that contains distinctive mineral assemblages. It is often the case that hydrated minerals and their anhydrous counterparts are compositionally very similar. Thus, elemental analyses would not easily distinguish one from the other. Mineralogical analysis, comprising both compositional and structural information, can provide a definitive answer.

6.5.6. Evidence of Extinct Life

Evidence of life on the Earth occurs in the earliest rocks that could have preserved signs of its presence ~3.5 b.y. ago. However, much of the geologic record from the earliest sedimentary sequences has either been heated to the extent that metamorphism would have removed evidence of life, or has simply been destroyed by subduction. Due to the apparent lack of tectonic activity on Mars, a great deal of the sediment deposited on the ancient martian surface still exists and was probably not heated to the extent of equivalent sediments on the early Earth. Therefore, it is likely that if life originated early in Mars history, some record of its existence would be manifest in the earliest geologic record.

REFERENCES

Abraham A. (1961) *The Principles of Nuclear Magnetism.* Oxford.

Abraham A. and Bleaney B. (1970) *Electron Paramagnetic Resonance of Transition Ions.* Clarendon, Oxford.

Adams J. B. and McCord T. B. (1969) Interpretation of spectral reflectivity of light and dark regions. *JGR, 74,* 4851–4856.

Adler H. H. and Kerr P. F. (1963) Infrared absorption frequency trends for anhydrous normal carbonates. *Am. Mineral., 48,* 124–137.

Agresti D. G. et al. (1992a) A backscatter Mössbauer spectrometer (BaMS) for use on Mars. In *Workshop on Innovative Instrumentation for the In Situ Study of Atmosphere-Surface Interactions on Mars* (B. Fegley Jr. and H. Wänke, eds.). LPI Tech. Rpt. 92-07, Part 1, LPI, Houston.

Agresti D. G. et al. (1992b) Development of a Mössbauer backscattering spectrometer, including X-ray fluorescence spectroscopy, for the in situ mineralogical analysis of the Mars surface. In *Workshop on Innovative Instrumentation for the In Situ Study of Atmosphere-Surface Interactions on Mars* (B. Fegley Jr. and H. Wänke, eds.). LPI Tech. Rpt. 92-07, Part 1, LPI, Houston.

Agresti D. G. et al. (1992c) Extraterrestrial Mössbauer spectroscopy. *Hyperfine Interact., 72,* 285–298.

Arnold G. and Wagner C. (1988) Grain-size influence on the mid-infrared spectra of the minerals. *Earth, Moon, Planets, 41,* 163–171.

Baird A. K. (1976) Mineralogic and petrologic implications of Viking geochemical result from Mars: Interim report. *Science, 194,* 1288–1293.

Barnes D. F. (1958) *Infrared Luminescence of Minerals.* USGS Bull. 1052-C.

Benz W. et al. (1988) Collisional stripping of Mercury's mantle. *Icarus, 74,* 516–528.

Bertin E. P. (1978) *Introduction to X-Ray Spectrometric Analysis.* Plenum, New York. 485 pp.

Bish D. L. and Chipera S. J. (1988) Problems and solutions in quantitative analysis of complex mixtures by X-ray powder diffraction. *Adv. X-Ray Anal., 31,* 295–308.

Bish D. L. and Howard S. A. (1986) Quantitative analysis via the Rietveld method. *Workshop on Quantitative X-Ray Diffraction Analysis.* National Bureau of Standards.

Bish D. L. and Howard S. A. (1988) Quantitative phase analysis using the Rietveld method. *J. Appl. Cryst., 21,* 86–91.

Bish D. L. and Post J. E. (1993) Quantitative mineralogical analysis using the Rietveld full-pattern fitting method. *Am. Mineral., 78,* 932–940.

Brindley G. W. (1980) Quantitative X-ray mineral analysis of clays. In *Crystal Structures of Clay Minerals and Their X-Ray Identification* (G. W. Brindley and G. Brown, eds.), pp. 411–438. Mineralogical Society.

Boynton W. (1994) A concept for a thermal and evolved gas analyzer for martian soils. In *Mars Surveyor Science Objectives and Measurements Requirements Workshop* (D. J. McCleese et al., eds.), p. 30. JPL Tech. Rept. D12017.

Burns R. G. (1988) Gossans on Mars. *Proc. Lunar Planet. Sci. Conf. 18th,* pp. 713–721.

Burns R. G. (1993) *Mineralogical Application of Crystal Field Theory,* 2nd edition. Cambridge Univ., Cambridge. 551 pp.

Burns R. G. (1993) Mössbauer spectral characterization of iron in planetary surfaces. In *Remote Geochemical Analysis: Elemental and Mineralogical Composition* (C. M. Pieters and P. A. J. Englert, eds.). Cambridge Univ.

Butler B. et al. (1993) Mercury: Full-disk radar images and the detection and stability of ice at the north pole. *JGR, 98,* 15003–15023.

Carr M. et al. (1995) *An Exobiological Strategy for Mars Exploration.* Prepared by the Exobiology Program Office, NASA HQ, January, 1995, NASA-SP-530.

Chase S. C. Jr. (1978) Viking Infrared Thermal Mapper. *Appl. Opt., 17,* 1243–1251.

Christensen P. R. and Harrison S. T. (1993) Thermal infrared emission spectra of natural surfaces: Application to desert varnish coatings on rocks. *JGR, 98,* 19819–19834.

Christensen P. R. et al. (1992) Thermal emission spectrometer experiment: Mars Observer mission. *JGR, 97,* 7719–7734.

Chung F. H. (1974a) Quantitative interpretation of X-ray diffraction patterns of mixtures. I. Matrix-flushing method of quantitative multicomponent analysis. *J. Appl. Cryst., 7,* 519–525.

Chung F. H. (1974b) Quantitative interpretation of X-ray diffraction patterns of mixtures. II. Adiabatic principle of X-ray diffraction analysis of mixtures. *J. Appl. Cryst., 7,* 526–531.

Clark B. E. et al. (1992) Meteorite-asteroid spectral comparison: The effects of comminution, melting, and recrystallization. *Icarus, 97,* 288–297.

Clark B. C. et al. (1982) Chemical composition of martian fines. *JGR, 87,* 10059–10068.

Clark R. N. et al. (1990) High-resolution reflectance spectra of Mars in the 2.3 micrometer region: Evidence for the mineral scapolite. *JGR, 95,* 14463–14480.

Clifford S. M. et al. (1988) *Scientific Results of the NASA-Sponsored Study Project Mars: Evolution of Its Climate and Atmosphere.* LPI Tech. Rpt. 88-09, LPI, Houston.

Compton R. R. (1962) *Manual of Field Geology.* Wiley, New York.

Conel J. E. (1969) Infrared emissivities of silicates: Experimental results and a cloudy atmosphere model of spectral emission from condensed particulate mediums. *JGR, 74,* 1614–1634.

Conrath B. et al. (1973) Atmospheric and surface properties of Mars obtained by infrared spectroscopy on Mariner 9. *JGR, 78,* 4267–4278.

Conrath B. J. (1975) Thermal structure of the martian atmosphere during the dissipation of the dust storm of 1971. *Icarus, 24,* 36–46.

Cronin J. R. et al. (1988) Organic matter in carbonaceous chondrites, planetary satellites, asteroids, and comets. In *Meteorites in the Early Solar System* (J. F. Kerridge and M. S. Matthews, eds.), pp. 819–857. Univ. of Arizona, Tucson.

Fanale F. P. and Cannon W. A. (1979) Mars: CO_2 absorption and capillary condensation on clays—Significance for volatile storage and atmospheric history. *JGR, 84,* 8404–8415.

Farmer V.C. (1974) *Infrared Spectra of Minerals.* Mineral Society, London. 539 pp.

Fegley B. Jr. and Treiman A. H. (1992) Chemistry of atmosphere-surface interactions on Venus and Mars. In *Venus and Mars: Atmospheres, Ionospheres, and Solar Wind* (J. G. Luhmann et al., eds.), pp. 7–71. AGU Geophysical Monograph 66.

Fry N. (1984) *The Field Description of Metamorphic Rocks.* Open Univ.

Geake J. E. and Walker G. (1975) Luminescence of minerals in the near-IR. In *Infrared and Raman Spectroscopy of Lunar and Terrestrial Minerals* (C. Karr Jr., ed.), pp. 73–90. Academic, New York.

Gillespie A. R. et al. (1984) Mapping alluvial fans in Death Valley, CA, using multichannel thermal infrared images. *Geophys. Res. Lett., 11,* 1153–1156.

Goettel K. A. (1988) Present bounds on the bulk composition of Mercury: Implications for Planetary Formation Processes. In *Mercury* (F. Vilas et al., eds.), pp. 613–621. Univ. of Arizona, Tucson.

Goetz A. F. H. (1967) Infrared 8–13 μm spectroscopy of the Moon and some cold silicate powders. Ph.D. thesis, Calif. Inst. Tech.

Goetz A. F. H. et al. (1982) Mineral identification from orbit: Initial results from the shuttle multispectral infrared radiometer. *Science, 218,* 1020–1024.

Goldsmith J. R. et al. (1961) Lattice constants of the calcium-magnesium carbonates. *Am. Mineral., 46,* 453–457.

Gooding J. L. (1978) Chemical weathering on Mars: Thermodynamic stabilities of primary igneous minerals (and their alteration products) from mafic igneous rocks. *Icarus, 33,* 483–513.

Gooding J. L. (1992) Soil mineralogy and chemistry on Mars: Possible clues from salts and clays in SNC meteorites. *Icarus, 99,* 28–41.

Gooding J. L. (1994) Martian soil water content and mineralogy determined by differential scanning calorimetry and evolved-gas analysis. In *Mars Surveyor Science Objectives and Measurements Requirements Workshop* (D. J. McCleese et al., eds.), pp. 68–69. JPL Tech. Rept. D12017.

Gooding J. L. and Keil K. (1978) Alteration of glass as a possible source of clay minerals on Mars. *Geophys. Res. Lett., 5,* 727–730.

Gooding J. L. et al. (1992) Physical and chemical weathering. In *Mars* (H. H. Kieffer et al., eds.), pp. 626–651. Univ. of Arizona, Tucson.

Griffith W. P. (1975) Raman spectroscopy of terrestrial minerals. In *Infrared and Raman Spectroscopy of Lunar and Terrestrial Minerals* (C. Karr Jr., ed.), pp. 299–324. Academic, New York.

Hall P. L. (1980) The application of electron spin resonance spectroscopy to studies of clay minerals, I and II. *Clay Minerals, 15,* 321–349.

Hanel R. A. et al. (1970) The Nimbus III Michelson interferometer. *Appl. Opt., 9,* 1767–1774.

Hanel R. et al. (1972) Investigation of the martian environment by infrared spectroscopy on Mariner 9. *Icarus, 17,* 423–442.

Hanel R. et al. (1980) *Appl. Opt., 19,* 1391.

Hapke B. (1981) Bidirectional reflectance spectroscopy I. Theory. *JGR, 86,* 3039–3054.

Hapke B. (1993) *Theory of Reflectance and Emittance Spectroscopy.* Cambridge Univ.

Harmon J. K. et al. (1994) Radar mapping of Mercury's polar anomalies. *Nature, 369,* 213–215.

Hill R. F. and Howard C. J. (1987) Quantitative phase analysis from neutron powder diffraction data using the Rietveld method. *J. Appl. Cryst., 20,* 467–474.

Hochella M. F. Jr. (1988) Auger electron and X-ray photoelectron spectroscopies. In *Spectroscopic Methods in Mineralogy and Geology* (F. C. Hawthorne, ed.). Mineral. Soc. Am.

Hovis W. A. Jr. and Callahan W. R. (1966) Infrared reflectance spectra of igneous rocks, tuffs, and red sandstone from 0.5 to 22 μ. *J. Opt. Soc. Am., 56,* 639–643.

Howard S. A. and Preston K. D. (1989) Profile fitting of powder diffraction patterns. In *Modern Powder Diffraction* (D. L. Bish and J. E. Post, eds.). Mineral. Soc. Am.

Hunt G. R. (1980) Electromagnetic radiation: The communication link in remote sensing. In *Remote Sensing in Geology* (B. S. Siegal and A. R. Gillespie, eds.), pp. 5–45. Wiley, New York.

Hunt G. R. and Logan L. M. (1972) Variation of single particle mid-infrared emission spectrum with particle size. *Appl. Opt., 11,* 142–147.

Hunt G. R. and Salisbury J.W. (1970) Visible and near-IR spectra of minerals and rocks: I. Silicate minerals. *Mod. Geol., 1,* 283–300.

Hunt G. R. et al. (1973) Mars: Components of infrared spectra and the composition of the dust cloud. *Icarus, 18,* 459–469.

Hunt G. R. and Salisbury J. W. (1974) *Mid-Infrared Spectral Behavior of Igneous Rocks.* Environ. Res. Paper, 496-AFCRL-TR-74-0625, p. 142.

Hunt G. R. and Salisbury J. W. (1975) *Mid-Infrared Spectral Behavior of Sedimentary Rocks.* Environ. Res. Paper, 520-AFCRL-TR-75-0356, p. 49.

Hunt G. R. and Salisbury J. W. (1976) *Mid-Infrared Spectral Behavior of Metamorphic Rocks.* Environ. Res. Paper, 543-AFCRL-TR-76-0003, p. 67.

Hunt G. R. and Vincent R. K. (1969) The behavior of spectral features in the infrared emission from particulate surfaces of various grain sizes. *JGR, 73,* 6039–6046.

Jakeš P. (1992) Analogue of hand-held lens and optical microscope for martian in situ studies (abstract). In *Workshop on Innovative Instrumentation for In Situ Study of Atmosphere-Surface Interaction on Mars* (B. Fegley Jr. and H. Wänke, eds.), p. 7. LPI Tech. Rpt. 92-07, Part 1, LPI, Houston.

Jakeš P. and Wänke H. (1993) Mikrotel microscope: An equivalent of hand held lens and optical microscope for "in situ" planetary (Mars) studies. Abstracts of Mars meeting, Wiesbaden, May 1993.

Jeanloz R. et al. (1995) Evidence for a basalt-free surface on Mercury and implications for internal heat. *Science*, in press.

Jones R. C. and Bish D. L. (1991) Quantitative X-ray diffraction analysis of soils: Rietveld full-pattern mineral concentrations and pattern curve fitting vs. P sorption of bauxite soils (abstract). *Proc. Ann. Clay Minerals Soc. Mtng., 28*, 84.

Kahle A. B. (1987) Surface emittance, temperature, and thermal inertia derived from thermal infrared multispectral scanner (TIMS) data for Death Valley, California. *Geophysics, 52*, 858–874.

Kahle A. B. and Goetz A. F. H. (1983) Mineralogic information from a new airborne thermal infrared multispectral scanner. *Science, 222*, 24–27.

Kahle A. B. et al. (1988) Relative dating of Hawaiian lava flows using multispectral thermal infrared images: A new tool for geologic mapping of young volcanic terranes. *JGR, 93*, 15239–15251.

Kankeleit E. et al. (1994) A Mössbauer experiment on Mars. *Hyperfine Interact., 90*, 107–120

Karr C. Jr., ed. (1975) *Infrared and Raman Spectroscopy of Lunar and Terrestrial Minerals*. Academic, New York. 375 pp.

Kastalsky V. and Westcott M. F. (1968) Accurate unit cell dimensions of hematite (-Fe_2O_3). *Austr. J. Chem., 21*, 1061–1062.

Kieffer H. H. Jr. et al. (1973) Preliminary report on infrared radiometric measurements from Mariner 9 spacecraft. *JGR, 78*, 4291–4312.

Kieffer H. H. et al. (1977) Thermal and albedo mapping of Mars during the Viking primary mission. *JGR, 82*, 4249–4292.

Kim S. S. and Bradley J. G. (1994) Characterization of martian surface chemistry by a miniature magnetic resonance spectrometer. In *Mars Surveyor Science Objectives and Measurements Requirements Workshop*, pp. 93–94. JPL, Pasadena.

Kittel C. (1948) On the theory of ferromagnetic resonance absorption. *Phys. Rev., 73*, 155–161.

Klingelhoefer G. et al. (1992) Mössbauer backscattering spectrometer for the mineralogical analysis of the Mars surface. *Hyperfine Interact., 71*, 1449–1452.

Klingelhoefer G. et al. (1995) Mössbauer spectroscopy in space. *Hyperfine Interact., 95*, 305–339.

Klug H. P. and Alexander L. E. (1974) *X-Ray Diffraction Procedures for Polycrystalline and Amorphous Materials*. Wiley, New York. 966 pp.

Knudsen J. M. et al. (1991) Mössbauer spectroscopy on the surface of Mars. Why? *Hyperfine Interact., 68*, 83–94.

Lazerev A. N. (1972) *Vibrational Spectra and Structure of Silicates*. Consultants Bureau, New York. 302 pp.

Logan L. M. et al. (1972) Compositional implications of Christiansen frequency maximums for infrared remote sensing applications. *JGR, 78*, 4983–5003.

Lyon R. J. P. (1962) *Evaluation of Infrared Spectroscopy for Compositional Analysis of Lunar and Planetary Oils*. Stanford. Res. Inst. Final Rep. Contract, NASA, 49(04).

Lyon R. J. P. (1964) *Evaluation of Infrared Spectrophotometry for Compositional Analysis of Lunar and Planetary Soils. II: Rough and Powdered Surfaces*. Stanford Research Institute, Palo Alto, CA, NTIS, NASA Contractor Report CR-100.

Mancinelli R. L. and White M. R. (1994) *In situ* identification of martian surface material using differential thermal analysis coupled to gas chromatography. In *Mars Surveyor Science Objectives and Measurements Requirements Workshop* (D. J. McCleese et al., eds.), pp. 112–113. JPL Tech. Rept. D12017.

Marfunin A. S. (1975) *Spectroscopy, Luminescence and Radiation Centers in Minerals*. Springer, New York.

Martin M. L. and Martin G. J. (1980) *Practical NMR Spectroscopy*. Heyden.

McBride M. B. (1990) Electron Spin Resonance Spectroscopy. In *Instrumental Surface Analysis of Geologic Materials* (D. L. Perry, ed.), pp. 233–281. VCH.

McCord T. B. (1982) Mars: Definition and characterization of global surface units with emphasis on composition. *JGR, 87*, 10129–10148.

McMillan P. F. and Hofmeister A. M. (1988) Infrared and Raman spectroscopy. In *Spectroscopic Methods in Mineralogy and Geology* (F. C. Hawthorne, ed.), pp. 99–160. Mineral. Soc. Am., Washington DC.

Miller S. L. (1973) The clathrate hydrates—their nature and occurrence. In *Physics and Chemistry of Ice*, pp. 42–50. Royal Society of Canada.

Miller S. L. and Smythe W. D. (1970) Carbon dioxide clathrate in the martian ice cap. *Science, 170*, 531–533.

Mitchell D. and de Pater I. (1994) Microwave imaging of Mercury's thermal emission at wavelengths from 0.3 to 20.5 cm. *Icarus, 110*, 2–32.

Moersch J. E. and Christensen P. R. (1991) Modeling particle size effects on the emissivity spectra of minerals in the thermal infrared (abstract). *BAAS, 23*.

Morgan T. H. et al. (1988) Impact-driven supply of sodium and potassium in the atmosphere of Mercury. *Icarus, 74*, 156–170.

Nash D. B. (1991) Infrared reflectance spectra (4–12 μm) of typical lunar samples. *Geophys. Res. Lett., 18*, 2145–2147.

Nash D. B. and Salisbury J. W. (1991) Infrared reflectance spectra (2.2–15 μm) of plagioclase feldspars. *Geophys. Res. Lett., 18,* 1151–1154.

Neugebauer G. et al. (1971) Mariner 1969 infrared radiometer results: Temperatures and thermal properties of the martian surface. *Astron. J., 76,* 719–728.

O'Connor B. H. and Raven M. D. (1988) Application of the Rietveld refinement procedure in assaying powdered mixtures. *Powder Diffr., 3,* 2–6.

Paige D. A. et al. (1992) The thermal stability of water ice at the poles of Mercury. *Science, 258,* 643–646.

Pearl J. C. (1983) Spatial variation in the surface composition of Io based on Voyager infrared data (abstract). *BAAS, 16,* 654.

Pieters C. M. and Englert P. A. J. (1993) *Remote Geochemical Analysis: Elemental and Mineralogical Composition.* Cambridge Univ., New York. 585 pp.

Pieters C. M. et al. (1995) Quantitative mineral analyses of planetary surfaces using reflectance spectroscopy. *Memorial Volume for R. G. Burns,* Geochemical Society, submitted.

Pinnavaia T. J. (1982) Electron spin resonance studies of clay minerals. In *Advanced Techniques for Clay Mineral Analysis* (T. J. Fripiat, ed.). Elsevier.

Pollack J. B. et al. (1987) The case for a wet warm climate on early Mars. *Icarus, 71,* 203–224.

Pollack J. B. et al. (1990) Simulations of the general circulation of the martian atmosphere, 1, Polar processes. *JGR, 95,* 1447–1474.

Pople J. A. et al. (1959) *High-Resolution Nuclear Magnetic Resonance.* McGraw-Hill.

Post J. E. and Bish D. L. (1989) Rietveld refinement of crystal structures using powder X-ray diffraction data. In *Modern Powder Diffraction* (D. L. Bish and J. E. Post, eds.), pp. 277–308. Mineral. Soc. Am.

Potter A. E. Jr. and Morgan T. H. (1981) Observations of silicate reststrahlen bands in lunar infrared spectra. *Proc. Lunar Planet. Sci. 12B,* pp. 703–713.

Prabhakara C. and Dalu G. (1976) Remote sensing of the surface emissivity at 9 μm over the globe. *JGR, 81,* 3719–3724.

Rado G. T. and Suhl H. (1963) *Magnetism, Vol. 1.* Academic, New York.

Rava B. and Hapke B. (1987) An analysis of the Mariner 10 color ratio map of Mercury. *Icarus, 71,* 387–429.

Salisbury J. W. and Eastes J. W. (1985) The effect of particle size and porosity on spectral contrast in the mid-infrared. *Icarus, 64,* 586–588.

Salisbury J. W. and Walter L. S. (1989) Thermal infrared (2.5–13.5 μm) spectroscopic remote sensing of igneous rock types on particulate planetary surfaces. *JGR, 94,* 9192–9202.

Schoen C. L. (1994) Fiber probes permit remote Raman spectroscopy. *Laser Focus World, 5,* 113–120.

Schwartz D. E. et al. (1995) Search for life on Mars: Evaluation of techniques. *Adv. Space Res., 15,* 193–197.

Settle M. (1979) Formation and depositon of volcanic sulfate aerosols on Mars. *JGR, 84,* 8343.

Sidorov Yu. I. and Zolotov M. Yu. (1986) Weathering of martian surface rocks. In *Chemistry and Physics of Terrestrial Planets* (S. K. Saxena, ed.), pp. 191–223. Springer Verlag, New York.

Singer R. B. (1982) Spectral evidence for the mineralogy of high-albedo soils and dust on Mars. *JGR, 87,* 10159–10168.

Slade M. et al. (1992) Mercury radar imaging: Evidence for polar ice. *Science, 258,* 635–640.

Slipher E. C. (1962) *The Photographic Atlas of Mars.* Sky Publishing, Cambridge, Massachusetts.

Smith W. H. (1992) COMPAS: Compositional mineralogy photoacoustic spectrometer (abstract). In *Workshop on Innovative Instrumentation for the In Situ Study of Atmosphere-Surface Interactions on Mars* (B. Fegley Jr. and H. Wänke, eds.), pp. 16–17. LPI Tech Rpt. 92-07, Part 1, LPI, Houston.

Snyder R. L. and Bish D. L. (1989). Quantitative analysis. In *Modern Powder Diffraction* (D. L. Bish and J. E. Post, eds.), pp. 101–144. Mineral. Soc. Am.

Sprague A. L. et al. (1994) Mercury: Evidence for anorthosite and basalt from mid-infrared (7.5–13.5 micrometer) spectroscopy. *Icarus, 109,* 156–167.

Thorpe R. and Brown G. (1985) *The Field Description of Igneous Rocks.* Wiley, New York.

Toon O. B. et al. (1977) Physical properties of the particles comprising the martian dust storm of 1971–1972. *Icarus, 3,* 663–696.

Toulmin P. et al. (1977) Geochemical and mineralogical interpretation of the Viking inorganic chemical results. *JGR, 82,* 4625–4634.

Treiman A. H. (1992) Optical luminescence spectroscopy as a probe of the surface mineralogy of Mars (abstract). In *Workshop on Innovative Instrumentation for in Situ Study of Atmosphere-Surface Interaction on Mars* (B. Fegley Jr. and H. Wänke, eds.), p. 17. LPI Tech. Rpt. 92-07, Part 1, LPI, Houston.

Treiman A. H. et al. (1993) Preterrestrial aqueous alteration of the Lafayette (SNC) meteorite. *Meteoritics, 28,* 86–97.

Tsay F. D. (1971) Ferromagnetic resonance of lunar samples. *GCA, 35,* 865–875.

Tucker M. E. (1982) *The Field Description of Sedimentary Rocks.* Wiley, New York.

Van der Marel H. W. and Beeutelspacher H. (1976) *Atlas of Infrared Spectroscopy of Clay Minerals and Their Admixtures.* Elsevier, Amsterdam. 396 pp.

Vilas F. et al. (1984) The dependence of reflectance spectra of Mercury on surface terrain. *Icarus, 59,* 60–68.

Vincent R. K. and Thompson F. (1972) Spectral compositional imaging of silicate rocks. *JGR, 17,* 2465–2472.

Vincent R. K. and Hunt G. R. (1968) Infrared reflectance from mat surfaces. *Appl. Opt., 7,* 53–59.

Vincent R. K. et al. (1975) Thermal-infrared spectra and chemical analyses of twenty-six igneous rock samples. *Remote Sens. Environ., 4,* 199–209.

Vonsovskii S. V. (1966) *Ferromagnetic Resonance.* Trans. by H. S. H. Massey and D. ter Haar. Pergamon.

Walter L. S. and Salisbury (1989) Spectral characterization of igneous rocks in the 8–12 μm region. *JGR, 94,* 9203–9213.

Walter M. R. and Des Marais D. J. (1993) Preservation of biological information in thermal spring deposits; developing a strategy for the search for fossil life on Mars. *Icarus, 101,* 129–143.

Wang A. et al. (1994) Database of standard Raman spectra of minerals and related inorganic crystals. *Appl. Spec., 48,* 959–968.

Waychunas G. A. (1988) Luminescence, X-ray emission, and new spectroscopies. In *Spectroscopic Methods in Mineralogy and Geology* (F. C. Hawthorne, ed.), pp. 639–698. Mineral. Soc. Am., Washington DC.

Wdowiak T. J. et al. (1995) A laser Raman system suitable for incorporation into lander spacecraft (abstract). In *Lunar and Planetary Science XXVI,* pp. 1473–1474.

Wendlandt W. W. (1986) *Thermal Analysis,* pp. 299–353. Wiley, New York.

Wertz J. E. and Bolton J. R. (1972) *Electron Spin Resonance, Elementary Theory and Practical Applications.* McGraw-Hill.

White W. B. (1975) Structural interpretation of lunar and terrestrial minerals by Raman spectroscopy. In *Infrared and Raman Spectroscopy of Lunar and Terrestrial Minerals* (C. Karr Jr., ed.), pp. 325–358. Academic, New York.

Wilson M. A. (1987) *NMR Techniques and Applications in Geochemistry and Soil Chemistry.* Pergamon.

Witteborn F. C. and Bregman J. (1984) A cryogenically cooled, multidetector spectrometer for infrared astronomy. *SPIE Cryo. Optical Syst. and Instr., 509,* 123–128.

Zolensky M. E. et al. (1988) Computer modeling of the mineralogy of the martian surface, as modified by aqueous alteration. In *Workshop on Mars Sample Return Science* (M. J. Drake et al., eds.), pp. 188–189. LPI Tech Rpt. 88-07, LPI, Houston.

APPENDIX 6.1. A TUNABLE DIODE LASER (TDL) SPECTROMETER AS A PLANETARY SURFACE INSTRUMENT

Albert Yen and Randy May

Tunable diode lasers (TDLs) are high-resolution (0.0005 cm^{-1}), near- to mid-IR sources that have been used for over 15 years in balloon and aircraft instruments to make absorption measurements of trace atmospheric constituents (*Webster et al.,* 1994). Traditional lead-salt TDLs operate between 3 and 30 μm but require cryogenic cooling (liquid He and N temperatures) and are, therefore, not practical for planetary surface experiments. Recent advances in semiconductor laser technology, however, allow operation at room temperature for wavelengths between 1.1 and 2.06 μm (Forouhar, 1986, personal communication). These new InGaAsP lasers are well suited for *in situ* evolved gas analyses of planetary surface samples and offer greater sensitivity (measurable absorptance of 0.001%) than existing mass spectrometry techniques for many species. Within the next year, GaSb-based TDLs operating between 2 and 5 m will become available and will provide additional flexibility in theselection of molecular transitions.

A planetary surface instrument for evolved gas analysis based on a TDL would consist of a laser, a detector for the operating wavelength (e.g., InGaAs), a thermoelectric cooler for temperature stabilization of the laser, control and data processing electronics, a sample collection mechanism, a heat source for volatilizing constituents in the sample, and an optical path between the laser and detector through the evolved gases. The wavelength scan range of a TDL is a few reciprocal centimeters and is typically achieved by applying a current ramp across the diode. Since temperature variations also affect the output wavelength of the laser, a thermoelectric cooler is necessary to maintain the TDL within approximately 0.1 K of a preselected set point. If the output of the TDL is modulated at a high frequency (typically kHz), then absorption sensitivities of 0.001% can be achieved by harmonic detection techniques using integration times of less than one second (*May and Webster,* 1993). Recent development work at JPL indicates that the TDL and its associated electronics can fit into a volume of less than 10 cm^3 and consume less than 1 W. The mass and volume of the overall instrument will be dominated by the design of the soil collector, optical chamber, heat source, etc. The power requirements will increase if electrical heating is used.

As a specific example, consider an evolved water analysis experiment for a Mars lander. A TDL operating at 7294 cm^{-1} would only need a 2.5-cm path from the laser to the detector to detect 15 ppmv of water vapor. If desired, a multipass (e.g., Herriott) cell could be used to increase the path length and lower the detection limit within a similar volume. Taking measurements every few seconds as the soil sample is heated would provide an evolved water signature. Additional TDLs scanning over different wavelengths could be used to quantify other evolved molecular species of interest (e.g., the isotopes of CO_2).

APPENDIX REFERENCES

Webster C. R. et. al. (1994) Aircraft Laser Infrared Absorption Spectrometer (ALIAS) for polar ozone chemistry on the ER-2. *Appl. Optics, 33,* 454–472.

Agrawal G. P. and Dutta N. K. (1986) *Long-Wavelength Semiconductor Lasers.* Van Nostrand Reinhold.

May R. D. and Webster C. R. (1993) Data processing and calibration for tunable diode laser harmonic absorption spectrometers. *J. Quant. Spectrosc. Radiat. Transfer, 49,* 335–347.